

ORIGINAL ARTICLE

DOI: <https://doi.org/10.18599/grs.2025.4.10>

Hydrodynamic Modeling of Complex Carbonate Reservoirs Considering Facies Zonality

S.N. Krivoshchekov*, A.A. Kochnev, E.S. Ozhgibesov, D.O. Shirinkin, A.L. Yuzhakov
Perm National Research Polytechnic University, Perm, Russian Federation

Abstract. Hydrodynamic modeling is an important stage in the design of rational development of oil fields. However, the process of model creation is accompanied by a large number of difficulties associated with the uncertainty of reservoir properties. This problem is especially relevant when modeling complex carbonate reservoirs. One of the key parameters required to create a hydrodynamic model are the dependences of relative phase permeabilities. The standard approach is to create single dependences of relative phase permeabilities for the whole reservoir. However, at such an approach the peculiarities of filtration in separate zones of the formation are minimized. Within the framework of this study we have created a hydrodynamic model of the field characterized by a complexly constructed carbonate reservoir, taking into account the facies zonality in determining the dependences of relative phase permeabilities. In the course of the work the laboratory studies were linked to different facies zones of the deposit. For each facies zone, approximation of relative phase permeability dependences was carried out using LET model. The distribution of selected facies in the hydrodynamic model by specifying different regions in a three-dimensional grid was carried out, and the loading of dependences of relative phase permeabilities by facies zones was also carried out. According to the modeling results, it was found that the use of separate dependencies of relative phase permeabilities for each facies zone increases the convergence of technological indicators of development with the historical trend compared to the standard approach. The study also included the design of geological and technological measures on the modified model taking into account facies zonality. The designed measures allowed for 10 years of forecast calculations to increase oil production by 5551.5 c.u. in comparison with the basic calculation, with practically unchanged watercut – 1.2%.

Keywords: complex carbonate reservoir, facies zonality, relative phase permeabilities, displacement coefficient, hydrodynamic model

Recommended citation: Krivoshchekov S.N., Kochnev A.A., Ozhgibesov E.S., Shirinkin D.O., Yuzhakov A.L. (2025). Hydrodynamic Modeling of Complex Carbonate Reservoirs Considering Facies Zonality. *Georesursy = Georesources*, 27(4), pp. 235–245. <https://doi.org/10.18599/grs.2025.4.10>

Introduction

Geological and hydrodynamic reservoir modeling is an integral part of rational planning of oil and gas field development. Hydrodynamic modeling makes it possible to reproduce field development processes, evaluate the efficiency of well-workover measures, and predict key development indicators (Gareeva, 2020).

However, the efficiency and predictive capability of models directly depend on the quality of the input data used (Arnold et al., 2016). The problem is particularly acute for complex carbonate reservoirs characterized by high uncertainty of properties due to their extreme geological heterogeneity. Factors that increase uncertainty include changes in depositional cycles, facies zonation, and the development of secondary alterations (Ryasnoy, Savelieva, 2019; Mahdaviara et al., 2021; Li et al., 2021; Tadayoni et al., 2020). Numerous studies are devoted to the structural complexity and modeling of carbonate reservoirs (Lucia et al., 2003; Masalmeh, Jing, 2007; Martin et al., 1997; Dominguez et al., 1992).

*Corresponding author: Sergey N. Krivoshchekov
 e-mail: krivoshchekov@gmail.com

© 2025 The Authors. Published by Georesursy LLC
 This is an open access article under the Creative Commons Attribution 4.0 License (<https://creativecommons.org/licenses/by/4.0/>)

Relative permeability (RP) is one of the key factors in reservoir modeling, indicating the ability of a porous medium to allow fluid flow. It forms the basis for calculating oil displacement efficiencies (Yekta et al., 2018). Based on RP, zones of single-phase oil flow, two-phase oil–water flow, and single-phase water flow are identified (McPhee et al., 2015).

RP functions can be obtained in different ways. The most widely used in practice are direct core studies by steady-state and unsteady-state displacement methods (Gubaydullin et al., 2017; Honarpour, Mahmood, 1988). In the absence of direct measurements, relative permeabilities may be evaluated analytically using various models (e.g. the Burdine model) based on laboratory capillary-pressure measurements (Honarpour et al., 1986). One of the disadvantages of laboratory core studies is the difference between the core plug size and the cell size in the reservoir model, which can lead to significant scale effects, particularly in complex reservoirs. Mikhaylov and Gurbatova (2012) demonstrated significant discrepancies between RP curves obtained from standard plugs and from full-diameter core samples in complex carbonate reservoirs. The authors note that the decisive factor controlling scale effects is the pore structure. Stepanov et al. (2024) proposed an approach for determining reservoir flow properties at the facies scale; this approach enabled a high degree of agreement between calculated and observed water-cut dynamics without any model tuning.

Another way to account for scale effects when estimating relative permeabilities is to use methods based on field data processing. These methods employ well performance data and specially designed well-testing and logging results. For example, Shurunov (2025) presents a method for determining RP that consists of deriving a total mobility curve from well-testing data and then splitting this curve into oil and water relative permeabilities by numerical simulation constrained by actual field performance. Zakirov et al. (2017) used a combination of hydrodynamic and well logging data to estimate RP: several injection–production cycles were carried out, during which dynamic wellhead and bottom-hole parameters were measured and water saturation was determined using pulsed neutron logging. However, approaches for determining RP from field data have not gained wide practical use; therefore, the standard practice remains the use of results from direct core flow experiments.

In a hydrodynamic model, core-derived RP curves were approximated. The most common models for approximating RP curves are the Corey model, the Sigmund and McCaffery model, the Kjøller (Kjerlich) model, and the LET model (Dubrovin et al., 2022; Lomeland, Orec, 2018).

A standard approach is to construct a single set of oil and water RP curves for the entire reservoir based on approximation of all available core data (Tudvachev, Konosavskiy, 2013). Under this approach, however, specific flow characteristics of local reservoir regions from which core was taken are averaged out.

To account for reservoir flow properties in more detail, it is relevant to use several RP functions for different reservoir zones. For example, Stepanenko (2018) assigned different RP functions to different lithological rock types. Shenawi et al. (2007) distributed relative permeabilities based on hydraulic flow units determined by the FZI (flow zone indicator) method.

Korovin (2021) proposed the use of different RP functions for individual lateral parts of a field with a terrigenous reservoir. It was shown that this approach allowed the calculated cumulative production to match the observed production more closely.

The objective of this study is to build a hydrodynamic model of a field with a complex carbonate reservoir, taking into account formation facies when defining RP functions.

Geology

The object of study is the Alpha field, located in the Timan–Pechora petroleum province. Petroleum deposits are confined to a complex carbonate reservoir. The facies architecture has been derived from seismic facies analysis using sequence-stratigraphic principles (Ladeyshchikov et al., 2022). Two high-frequency (fourth-order) sequences are distinguished in the studied area, formed during the Late Devonian time (Zadonsky and Yelets stages). Oil accumulations are associated with these deposits. The Zadonsky reef was formed within a single stratigraphic cycle, whereas the Yelets reef developed within three reef-building cycles. The main reef-building phase occurred during the highstand systems tract (HST), which is characterized by maximum accommodation space and optimal solar radiation and oxygen supply to support efficient photosynthesis by reef-building organisms.

Reef buildups extend in a relatively narrow belt from the southeast to the northwest. To the west, the reef trend passes into a shallow-water reef shelf. To the east, the reef margin passes into the fore-reef slope of the carbonate platform, which grades into a deep-water shelf. Lateral positions of reef buildups of different cycles are generally similar, except for the second reef-building cycle D3fm1(el), whose reefs have only limited areal extent within the area.

Materials and methods

The data set used in this study consists of measured RP curves. In total, 46 RP measurements were analyzed.

In this study, the obtained data were divided into two contrasting facies groups:

- barrier reef facies group (reef buildup, reef apron);
- back-reef shelf facies group (shallow shelf).

The distribution of measurements by facies group is given in Table 1.

Due to the absence of RP measurements for the second reef-building cycle $D_3fm_1(el)$ and the limited areal extent of reefs of this cycle within the field, RP functions for these deposits were assumed to be identical to those of the barrier-reef facies group of the third reef-building cycle.

Approximation of the measured RP values was performed using the LET model. Water and oil RP were approximated using equations (1) and (2), respectively:

$$f_{wi}(S_{wni}) = f_w^* \frac{(S_{wni})^{L_w}}{(S_{wni})^{L_w} + E_w \cdot (1 - S_{wni})^{T_w}}, \quad (1)$$

$$f_{oi}(S_{wni}) = f_o^* \frac{(1 - S_{wni})^{L_o}}{(1 - S_{wni})^{L_o} + E_o \cdot (S_{wni})^{T_o}}, \quad (2)$$

where S_{wni} is normalized water saturation; $f_{oi}(S_{wni})$ is the oil RP as a function of normalized water saturation S_{wni} ; $f_{wi}(S_{wni})$ is the water RP as a function of normalized water saturation S_{wni} ; f_o^* is the oil relative permeability at residual water saturation; f_w^* is the water RP at residual oil saturation; and L , E and T are the LET model correlation parameters for oil(o) and water(w) RP.

Normalized water saturation is calculated using equation (3):

$$S_{wni} = \frac{S_{wi} - S_{wr}}{1 - S_{or} - S_{wr}}, \quad (3)$$

where S_{wni} is normalized water saturation; S_{wi} is the water saturation; S_{wr} is residual water saturation; S_{or} is residual oil saturation.

Normalization of water relative permeability is carried out according to equation (4):

$$f_{wni}(S_{wni}) = \frac{f_{wi}(S_{wni})}{f_w^*}, \quad (4)$$

where $f_{wni}(S_{wni})$ is normalized water relative permeability; $f_{wi}(S_{wni})$ is the water relative permeability as a function of water saturation S_{wni} ; f_w^* is water relative permeability at residual oil saturation.

Normalization of oil relative permeability is carried out according to equation (5):

$$f_{oni}(S_{wni}) = \frac{f_{oi}(S_{wni})}{f_o^*}, \quad (5)$$

where $f_{oni}(S_{wni})$ is normalized oil relative permeability; $f_{oi}(S_{wni})$ is the oil relative permeability as a function of water saturation S_{wni} ; f_o^* is the oil relative permeability at residual water saturation.

Results

Study of RP and displacement coefficients for different facies types

For each facies group in each reef-building cycle, individual RP functions were constructed. Figure 1 shows RP curves for the facies groups in the Zadonsky deposits.

Analysis of the measured RP data for the barrier-reef facies group of the first reef-building cycle $D_3fm_1(el)$ shows significant heterogeneity in the values (Fig. 2). Therefore, the initial data were split into two groups by a threshold in absolute permeability (K_{abs}). To define the optimal threshold between the groups, a compactness metric was calculated for all possible permeability thresholds in the feature space consisting of residual oil saturation, residual water saturation and porosity. Compactness characterizes how closely observations in each group are clustered (Vashakidze et al., 2024); the smaller this metric, the better the separation between groups. Compactness was calculated using equation (6):

$$K = \sum_{j=1}^M \sum_{i=1}^N \|x_i^{(j)} - c_j\|^2, \quad (6)$$

where $\|x_i^{(j)} - c_j\|$ is the distance between an object and the group centroid, N is the number of elements in a group, and M is the number of groups. Prior to calculation, the features were normalized. The optimal permeability threshold of 12 mD was determined from the minimum value of the compactness metric (Fig. 3).

Calculated RP curves for the facies groups of the first reef-building cycle $D_3fm_1(el)$ are shown in Figure 4.

Relative permeabilities for the facies groups of the third reef-building cycle $D_3fm_1(el)$ are presented in Figure 5.

Reef-building cycle	Facies group	Number of measurements
$D_3fm_1(zd)$	barrier reef	1
	back-reef shelf	1
$D_3fm_1(el)$ (first reef-building cycle)	barrier reef	21
	back-reef shelf	3
$D_3fm_1(el)$ (third reef-building cycle)	barrier reef	11
	back-reef shelf	9

Table 1. Distribution of RP measurements by facies group

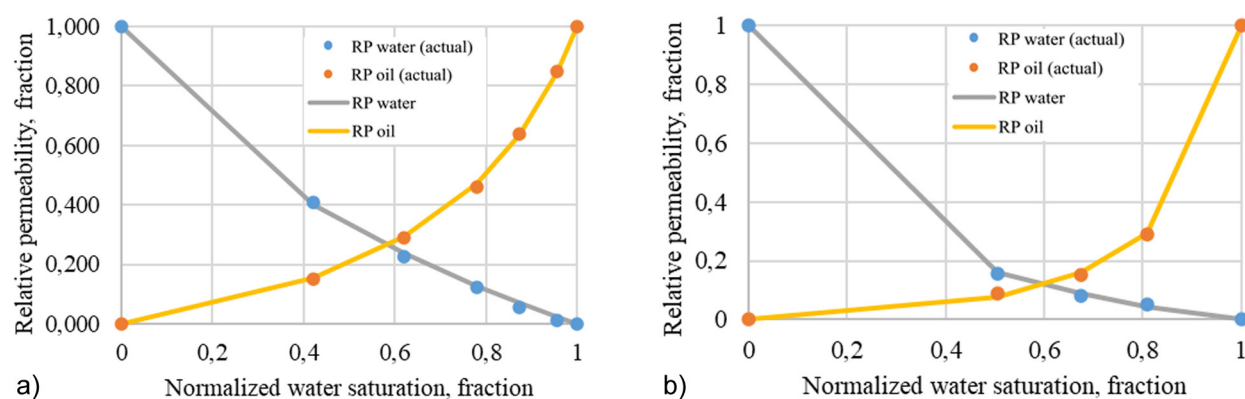


Figure 1. Relative permeabilities for facies groups in the Zadonsky deposits: (a) reef buildup; (b) back-reef shelf

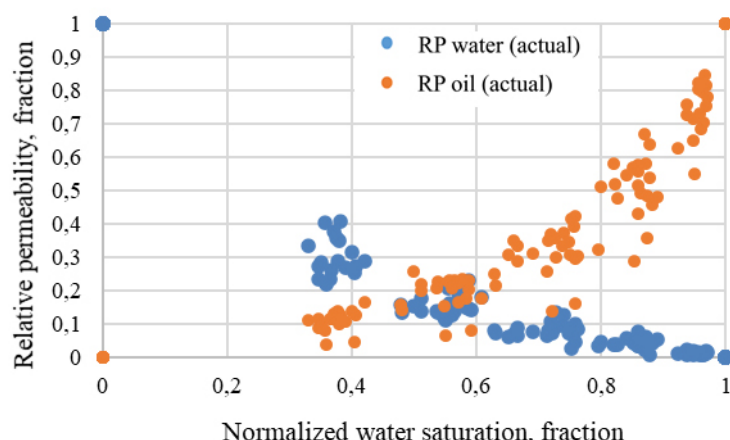


Figure 2. Measured relative permeability data for the barrier-reef facies group of the first reef-building cycle D3fm1(el)

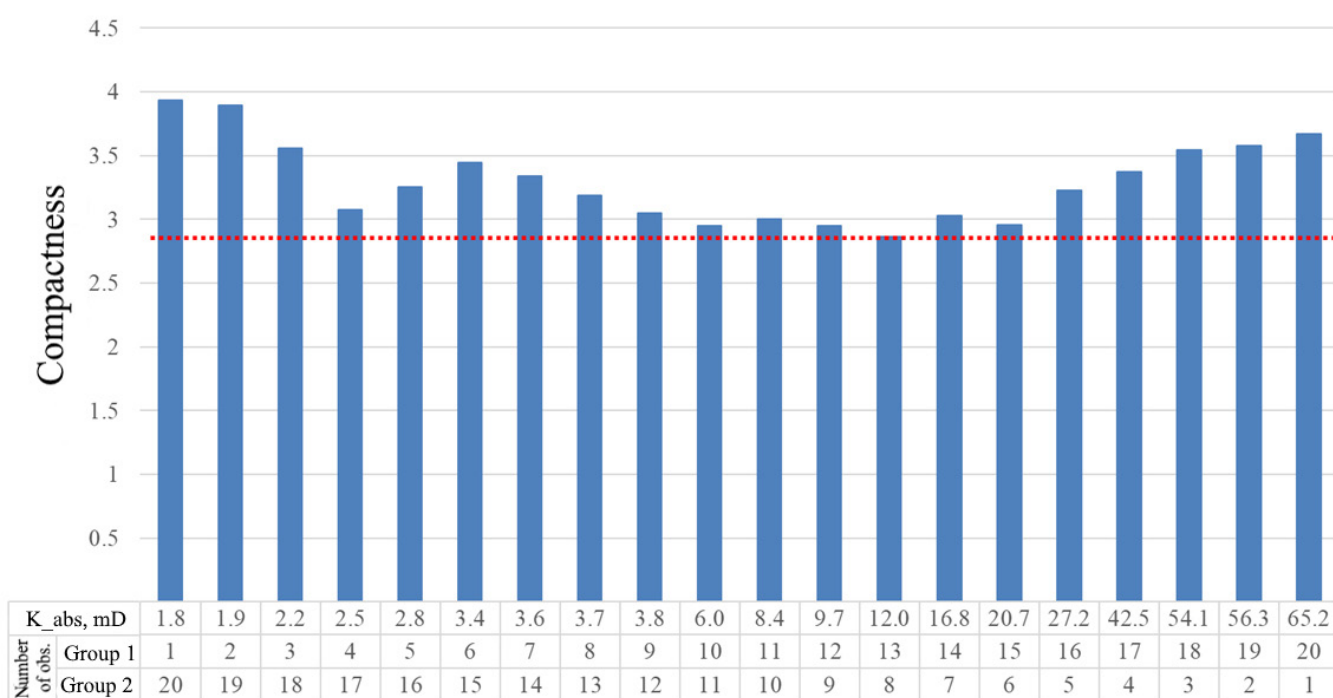


Figure 3. Determination of the optimal permeability threshold

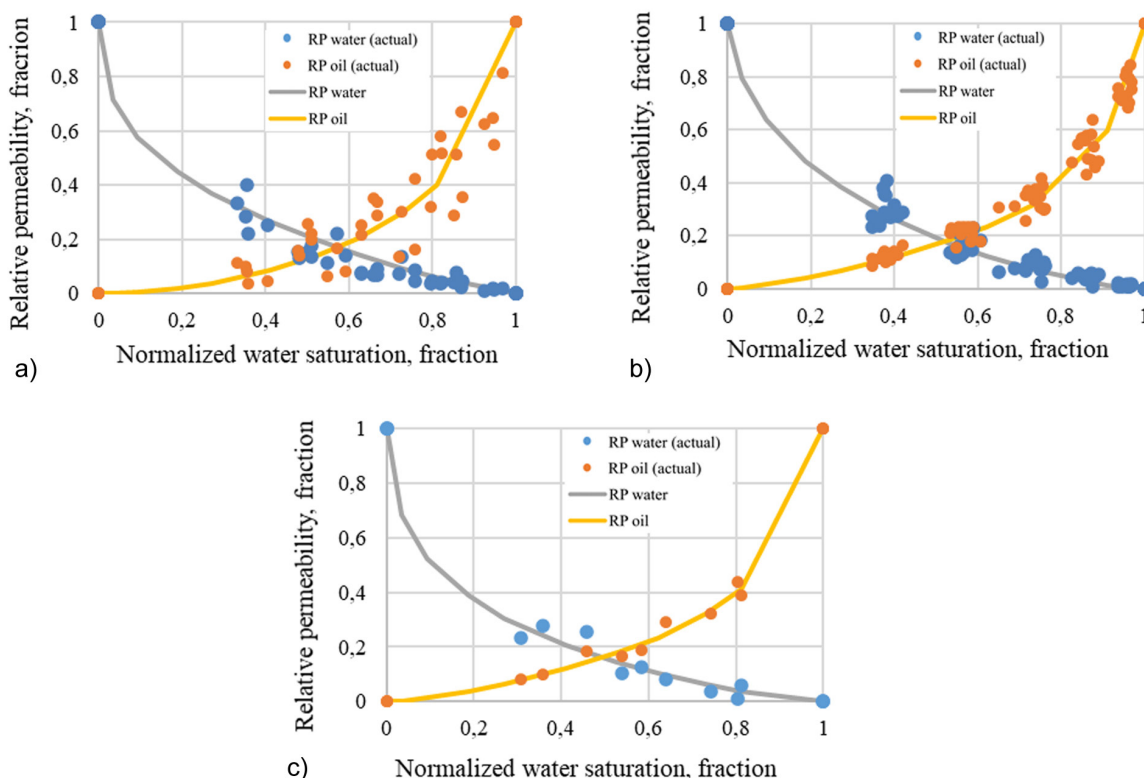


Figure 4. Relative permeabilities for the facies groups of the first reef-building cycle D3fm1(el): (a) barrier-reef group with $K_{abs} > 12$ mD; (b) barrier-reef group with $K_{abs} < 12$ mD; (c) back-reef shelf facies group

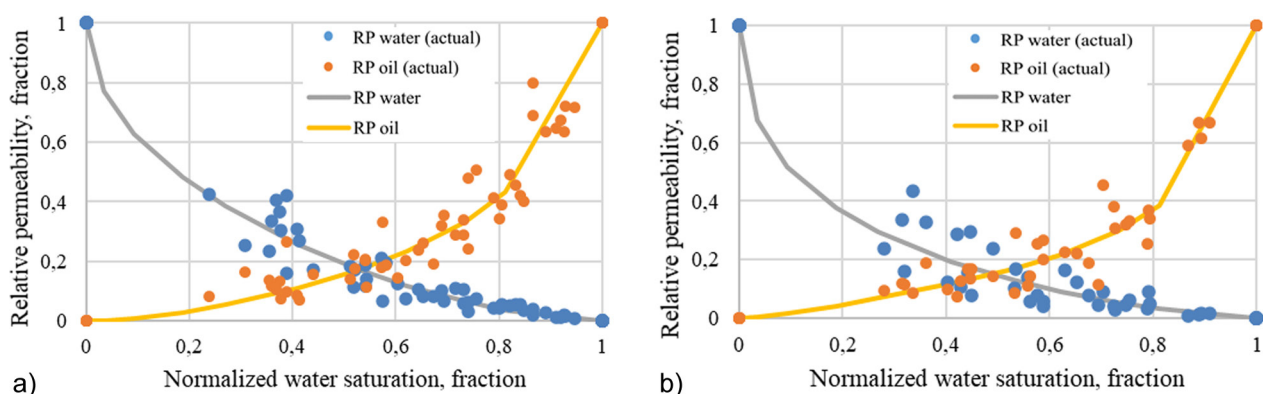


Figure 5. Relative permeabilities for the facies groups of the third reef-building cycle D3fm1(el): (a) barrier-reef group; (b) back-reef shelf facies group

Previous studies by Shirinkin (2021, 2022) showed that wells located within the barrier-reef facies group have significantly higher oil rates than wells within the back-reef shelf group. It was also noted that barrier-reef reservoirs have better petrophysical properties than back-reef shelf reservoirs.

In the next step, the endpoint relative permeabilities of the RP curves – residual oil saturation (S_{owcr}) and residual water saturation (S_{wscr}) – were determined for each facies group by averaging the measured data. Based on these data, displacement coefficients were calculated for each facies group.

The results are summarized in Table 2.

Table 2 shows that back-reef shelf facies are characterized by higher displacement coefficients than barrier-reef facies. In the Zadonsky and first Yelets reef-building cycles, the higher displacement coefficients in the back-reef shelf group are explained by reduced residual water saturation as a result of increased hydrophobicity of reservoirs. In the third Yelets reef-building cycle, the difference in displacement coefficients is due to higher residual oil saturation in the barrier-reef facies group.

Reef-building cycle	Facies group	Swcr, fraction	Sowcr, fraction	Displacement coefficient, fraction
D ₃ fm ₁ (zd)	Barrier reef	0.309	0.402	0.419
	Back-reef shelf	0.05	0.41	0.57
D ₃ fm ₁ (el) (first reef-building cycle)	Barrier reef (K _{abs} > 12 mD)	0.14	0.4	0.54
	Barrier reef (K _{abs} > 12 mD)	0.279	0.393	0.46
	Back-reef shelf	0.1	0.39	0.56
D ₃ fm ₁ (el) (third reef-building cycle)	Barrier reef	0.12	0.42	0.52
	Back-reef shelf	0.14	0.39	0.55

Table 2. Displacement coefficients by facies group

Reservoir modeling based on facies zonation

In the next stage, a facies cube was constructed. To this end, the three-dimensional grid in the hydrodynamic simulation model was subdivided according to the identified depositional cycles. Within each depositional cycle, facies groups were distributed according to facies-zonation schemes by assigning different regions in the model. A cross-section through the resulting facies cube is shown in Figure 6.

Using the same approach, cubes of endpoint saturations (Swcr and Sowcr) were built and populated by facies group.

The calculated RP functions for each facies group were then used in the hydrodynamic model, and history matching was carried out. It should be noted that the

field is developed with reservoir pressure maintenance by peripheral waterflooding.

To evaluate the quality of the history match for the Alpha field, model results using facies-based relative permeabilities were compared with a model using standard relative permeabilities and with actual field performance (Figs. 7, 8 and Table 3). For a consistent comparison, simulation results are presented after a single iteration.

It was established that using separate RP functions for each facies group yields better agreement with the historical trend in annual oil and liquid production than using standard relative permeabilities. With standard relative permeabilities, the simulated water-cut dynamics exceed the observed values, while cumulative liquid production is underpredicted (by 18.2% relative to the historical data).

- D₃fm₁(el)_3rd cycle_Back-reef shelf
- D₃fm₁(el)_3rd cycle_Barrier reef
- D₃fm₁(el)_2nd cycle_Barrier reef
- D₃fm₁(el)_1st cycle_Back-reef shelf
- D₃fm₁(el)_1st cycle_Barrier reef (K_{abs} > 12 mD)
- D₃fm₁(el)_1st cycle_Barrier reef (K_{abs} < 12 mD)
- D₃fm₁(zd)_Back-reef shelf
- D₃fm₁(zd)_Barrier reef

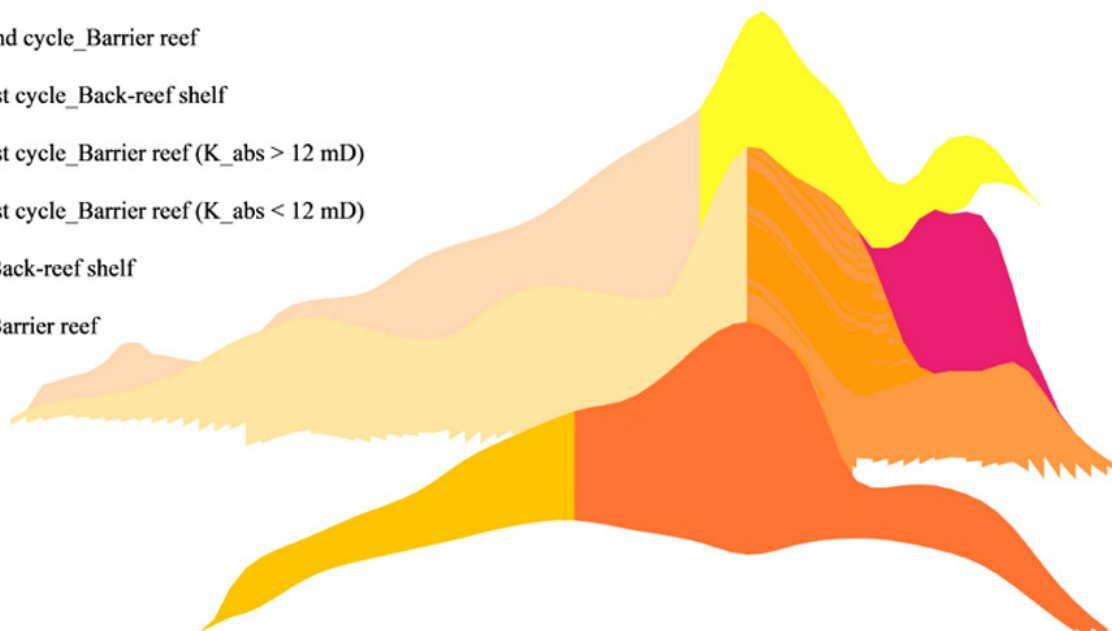


Figure 6. Cross-section through the facies cube for the Alpha field

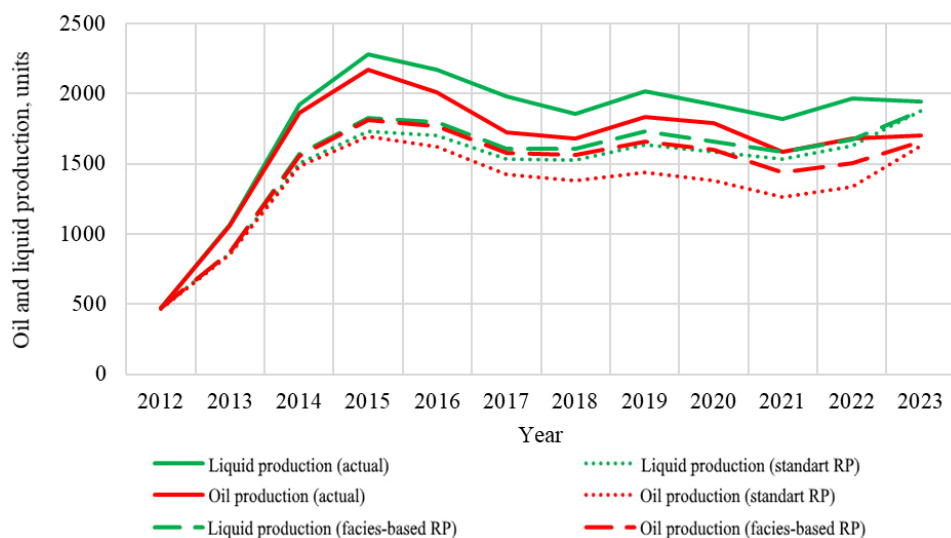


Figure 7. Comparison of oil and liquid production dynamics during history matching in the reservoir model

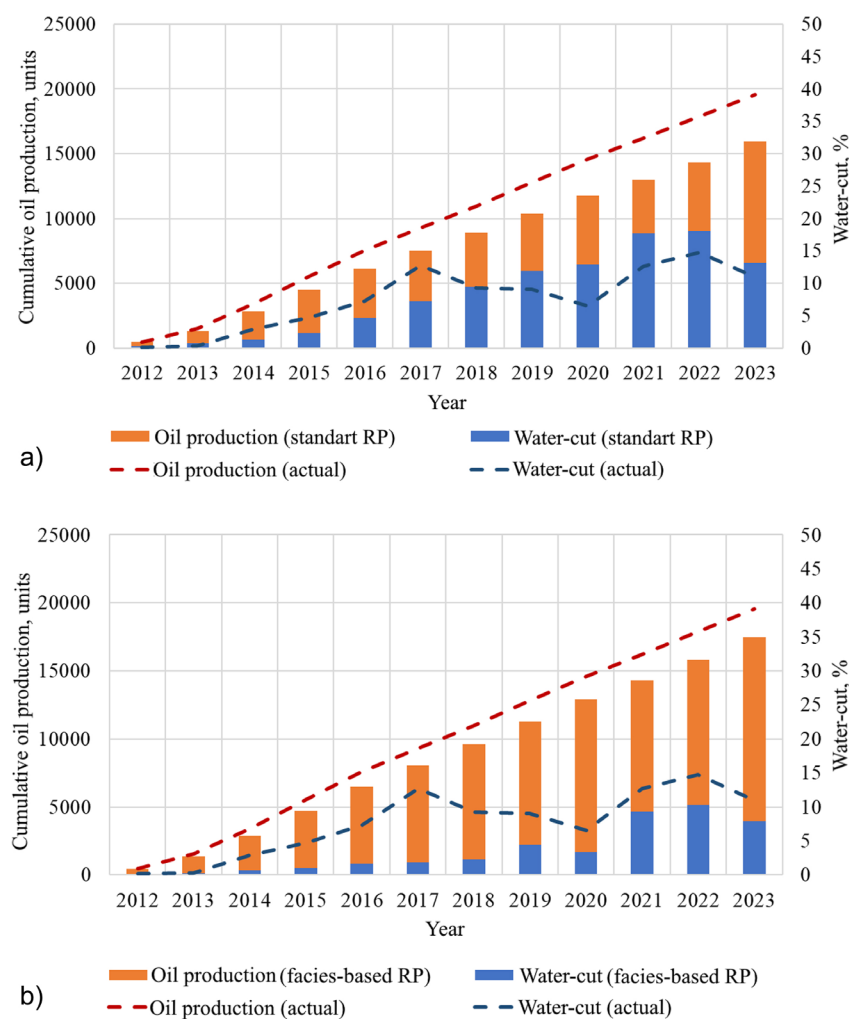


Figure 8. Comparison of cumulative oil production and water-cut dynamics during history matching in the reservoir model: (a) standard relative permeabilities; (b) facies-based relative permeabilities

Relative permeability specification	Cumulative liquid production, units	Cumulative oil production, units	Deviation of cumulative liquid from history, %	Deviation of cumulative oil from history, %
Facies-based	18267.6	17466.0	-15.1	-11.7
Standard	17591.1	15975.9	-18.2	-19.2
History	21516.3	19773.1		

Table 3. Comparison of cumulative indicators during history matching in the hydrodynamic model

When facies-based relative permeabilities are used, premature water breakthrough is absent, and cumulative liquid and oil production exhibit significantly better agreement with the production data of the Alfa oilfield.

Planning of production drilling and sidetracks

Before starting forecast calculations, the model with facies-based relative permeabilities, which showed the best agreement with historical data, was further history-matched to improve its predictive capability.

In the next step, a density map of residual oil in place was derived from hydrodynamic model and then compared with the facies maps. Based on the combined

maps (Fig. 9), the most favorable drilling targets were defined: zones of high residual oil density located within facies with superior flow properties (barrier-reef facies group).

Using this approach to locate production wells and sidetracks, a forecast was calculated with the hydrodynamic model of the Alpha field. Figures 10 and 11 and Table 4 show the forecast results.

As a result of using the proposed methodology for planning production drilling and well-workover measures, the 10-year forecast shows an increase in oil production of 5 551,5 units relative to the base case, with water cut remaining practically unchanged (only a 1,2% increase).

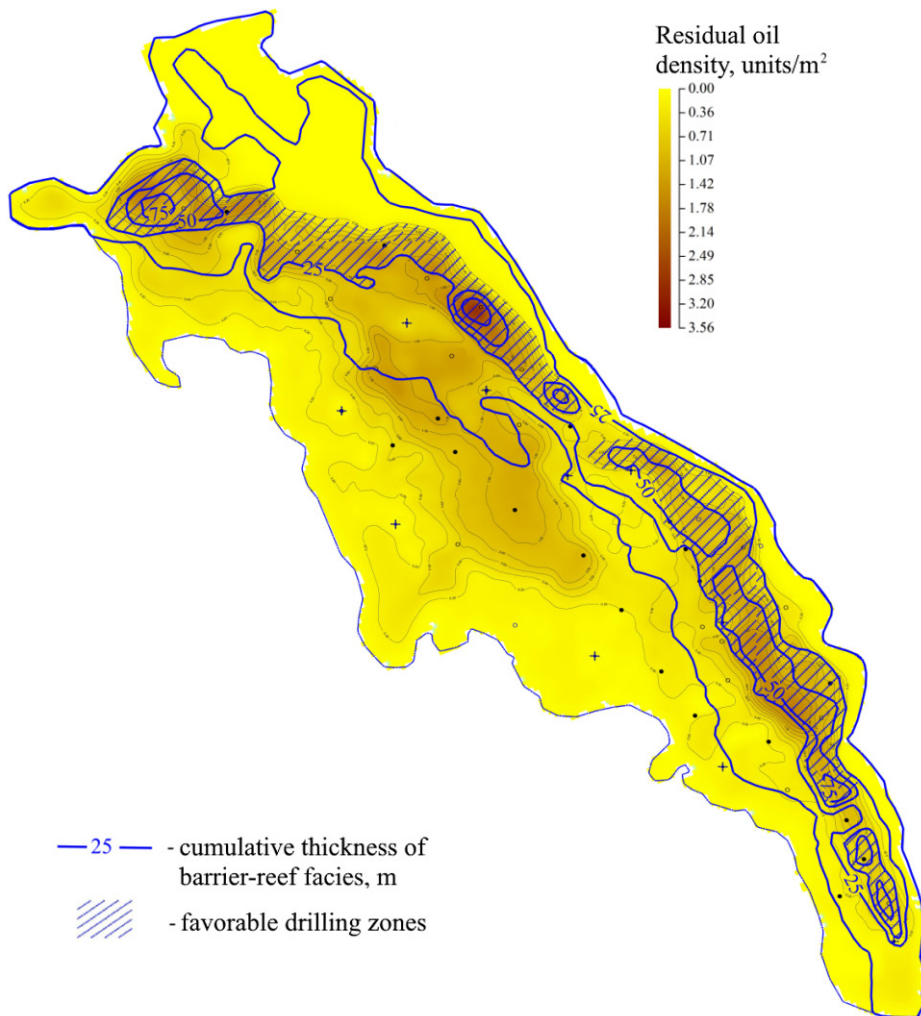


Figure 9. Comparison of the residual oil density map with the cumulative thickness of barrier-reef facies

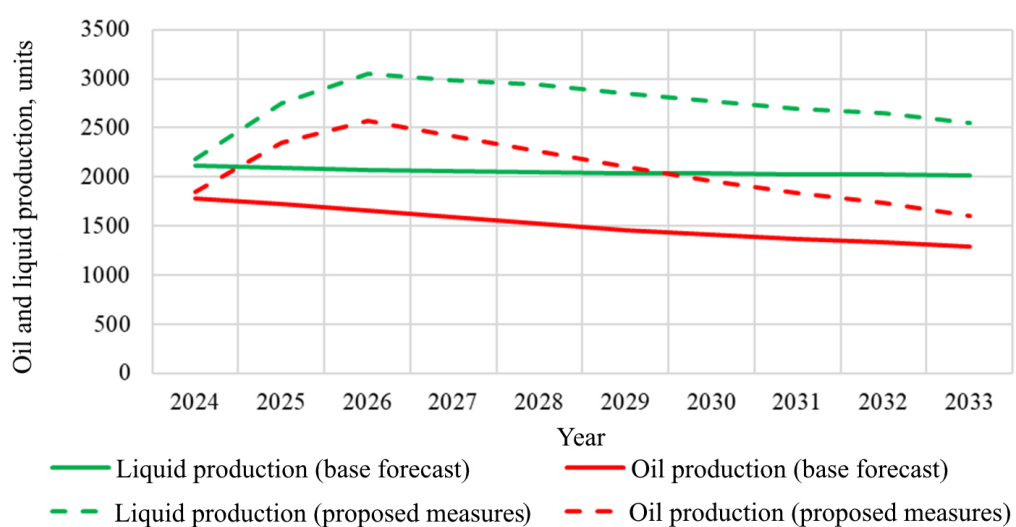


Figure 10. Comparison of forecast liquid and oil production dynamics for the base development scheme and the case with additional well-workover measures

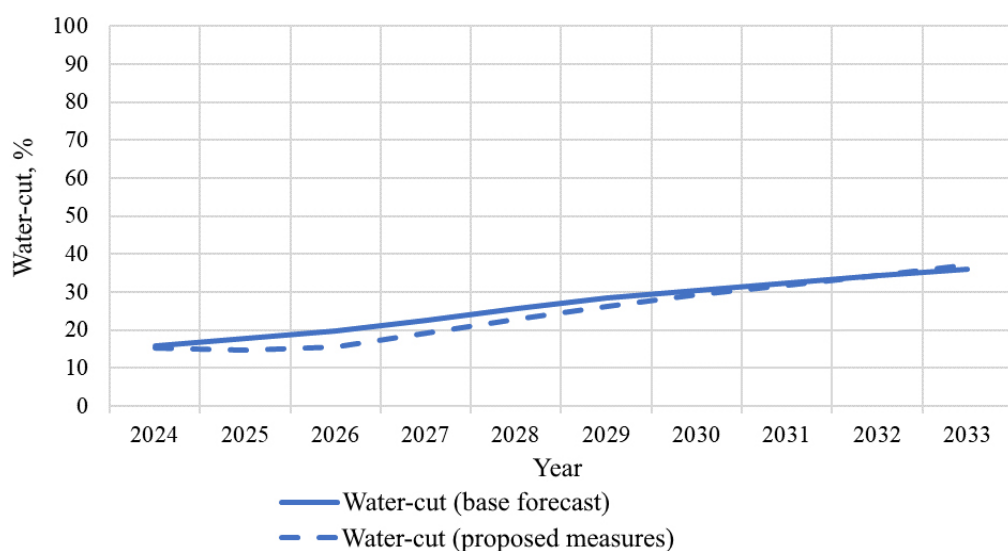


Figure 11. Comparison of forecast water-cut dynamics for the base development scheme and the case with additional well-workover measures

Forecast case	Cumulative liquid production, units	Cumulative oil production, units	Water cut, %
Base forecast	20521.1	15140.8	35.9
Forecast with proposed measures	27419.2	20692.3	37.1
Additional production / change in water cut	+6898.1	+5551.5	+1.2

Table 4. Comparison of cumulative indicators over 10 years of forecast for the base development scheme and with additional well-workover measures

Conclusion

The paper demonstrates the application of a modeling methodology that explicitly accounts for facies zonation in fields with complex reservoirs, using the Alpha field as an example.

An analysis of the facies zonation of the field was carried out, in which two different facies groups were identified in each reef-building cycle: a barrier-reef facies group and a back-reef shelf facies group. RP measurements were assigned to facies groups, and then were approximated using the LET model.

The identified facies groups were distributed in the hydrodynamic model by defining different regions in the three-dimensional grid; facies-based RP functions were then used to perform production history matching. It was shown that using RP functions defined for each facies group provides better agreement with the historical trend than using standard relative permeabilities: the deviations in cumulative liquid and oil production were reduced from -18.2% to -15.1% and from -19.1% to -11.7% , respectively.

Using the history-matched hydrodynamic model, a residual oil density map was constructed and, together with facies zonation maps, was used to plan development drilling and additional production measures. The proposed methodology resulted in an increase in oil production of 5 551,5 units over a 10-year forecast period relative to the base case, with water cut remaining practically unchanged (a 1.2% increase).

Acknowledgements

The research was funded by the Ministry of Science and Higher Education of the Russian Federation (Project No. FSNM-2023-0005).

References

Arnold D., Demyanov V., Christie M., Bakay A., Gopa K. (2016). Optimisation of decision making under uncertainty throughout field lifetime: A fractured reservoir example. *Computers & Geosciences*, 95, pp. 123–139. <https://doi.org/10.1016/j.cageo.2016.07.011>

Dominguez G. C., Fernando S. V., Chilingarian G. V. (1992). Simulation of carbonate reservoirs. *Developments in petroleum science*, 30, pp. 543–588. [https://doi.org/10.1016/S0376-7361\(09\)70135-9](https://doi.org/10.1016/S0376-7361(09)70135-9)

Dubrovin M. G., Vokina V. R., Yadryshnikova O. A. (2022). On the application of LET-model for approximation of core relative phase permeabilities. *Tyumen State University Herald. Physical and Mathematical Modeling. Oil, Gas, Energy*, 8(4), pp. 144–162. (In Russ.) <https://doi.org/10.21684/2411-7978-2022-8-4-144-162>

Gareeva A.A. (2020). Significance of geological and hydrodynamic modeling in the development and operation of oil and gas fields. *Actual researches*, 22, pp. 68–70. (In Russ.)

Gubaiddullin, M. G., Yuryev A. V., Belozerov I. P. (2017). Experimental studies of relative phase permeabilities and oil-water displacement coefficients in complexly constructed reservoirs. *Geology, Geophysics and Development of Oil and Gas Fields*, 2, pp. 49–52. (In Russ.)

Honarpour M., Koederitz L., Harvey A.H. (1986). Relative Permeability of Petroleum Reservoirs. Boca Raton: CRC Press., 152 p. <https://doi.org/10.1201/9781351076326>

Honarpour M., Mahmood S.M. (1988). Relative-permeability measurements: An overview. *Journal of petroleum technology*, 40(8), pp. 963–966. <https://doi.org/10.2118/18565-PA>

Korovin, M.O. (2021). Accounting for the influence of relative phase permeabilities on the adaptation of a field with terrigenous reservoir type. *Bulletin of the Tomsk Polytechnic University. Geo Assets Engineering*, 332(4), pp. 173–180. (In Russ.) <https://doi.org/10.18799/24131830/2021/4/3161>

Ladeyshchikov S.V., Fadeev A.P., Dorofeev N.V., Sabelnikov I.S., Zhemchugova T.A., Yuzhakov A.L. (2022). An integrated approach to creating three-dimensional geological models using the example of Timan-Pechora region fields. *Drilling and Oil*, 12, pp. 14–21. (In Russ.)

Li R., Chen Q., Deng H., Fu M., Hu L., Xie X., Zhang L., Guo X., Fan H., Xiang Z. (2021). Quantitative evaluation of the carbonate reservoir heterogeneity based on production dynamic data: A case study from Cretaceous Mishrif formation in Halfaya oilfield, Iraq. *Journal of Petroleum Science and Engineering*, 206, 109007. <https://doi.org/10.1016/j.petrol.2021.109007>

Lomeland F., Orec A. S. (2018). Overview of the LET family of versatile correlations for flow functions. *Proceedings of the International Symposium of the Society of Core Analysts*, 27–30 August 2018, Trondheim, Norway. <https://www.jgmaas.com/SCA/2018/SCA2018-056.pdf>

Lucia F. J., Kerans C., Jennings J. W. (2003). Carbonate reservoir characterization. *Journal of Petroleum Technology*, 55, pp. 70–72. <https://doi.org/10.2118/82071-JPT>

Mahdaviara M., Rostami A., Keivaniemehr F., Shahbazi K. (2021). Accurate determination of permeability in carbonate reservoirs using Gaussian Process Regression. *Journal of Petroleum Science and Engineering*, 196, 107807. <https://doi.org/10.1016/j.petrol.2020.107807>

Martin A. J., Solomon S. T., Hartmann D. J. (1997). Characterization of petrophysical flow units in carbonate reservoirs. *AAPG Bulletin*, 81, pp. 734–759. <https://doi.org/10.1306/522B482F-1727-11D7-8645000102C1865D>

Masalmeh S. K., Jing X. D. (2007). Improved characterisation and modelling of carbonate reservoirs for predicting waterflood performance. *Proceedings of the International Petroleum Technology Conference*, Dubai, U.A.E., 4–6 December 2007. <https://doi.org/10.2523/IPTC-11722-MS>

McPhee C., Reed J., Zubizarreta I. (2015). Core analysis: a best practice guide. Elsevier, 540 p.

Mikhailov N.N., Gurbatova I.P. (2012). Experimental study of the influence of scale effects on the characteristics of two-phase filtration. *Georesources. Geoenergetics. Geopolitics*, 1(5), pp. 1–3. (In Russ.)

Ovcharov V.V. (2014). Review of calculation methods and correction procedures of relative phase permeability curves for hydrodynamic modeling of hydrocarbon deposits. *Vestnik cybernetiki*, 1(13), pp. 10–16. (In Russ.)

Pozdnyakov A.A., Koreshkov R. B. (2011). Determination of two-phase filtration characteristics from field data. *Izvestiya vuzov. Neft i gas*, 4, pp. 60–65. (In Russ.)

Ryasnay A.A., Savelyeva E.N. (2019). Influence of secondary processes on the reservoir properties of carbonate rocks of the Vereiskiy oil and gas bearing complex (North-West of the Republic of Bashkortostan). *Regional Geology and Metallogeny*, 77, pp. 27–39. (In Russ.)

Shenawi S.H., White J.P., Elrafie E.A., El-Kilany K.A. (2007). Permeability and Water Saturation Distribution by Lithologic Facies and Hydraulic Units: A Reservoir Simulation Case Study». *Proceedings of the SPE Middle East Oil and Gas Show and Conference*, Manama, Bahrain, 11–14 March 2007. <https://doi.org/10.2118/105273-MS>

Shirinkin D.O. (2021) Analysis of the influence of facies structure on the development and operation of the East Lambeyshor field of the Timan-Pechora province. *Problems of development of hydrocarbon and ore mineral deposits*, 1, pp. 67–71. (In Russ.)

Shirinkin D.O. (2022) Analysis of heterogeneity of filtration-capacitive properties of the formation of the Yelets deposit of the East-Lambeyshorskoye field. *Proc. Oil and Gas Conference*, Moscow, 25–29 April 2022. (In Russ.)

Shurunov A.V. (2025). Determination of parameters of dependences of relative phase permeabilities using hydrodynamic studies of wells and numerical modeling for a low-permeability terrigenous reservoir. *Actual problems of oil and gas*, 16(1), pp. 24–35. (In Russ.) <https://doi.org/10.29222/ipng.2078-5712.2025.05>

Stepanenko, A.A. (2018). Practical techniques of hydrodynamic modeling. *Geology, Geophysics and Development of Oil and Gas Fields*, 9, pp. 41–45. (In Russ.) <https://doi.org/10.30713/2413-5011-2018-9-41-45>

Stepanov S.V., Lopatina E.S., Zagorovsky M.A., Zubareva I.A. (2024). Multiscale modeling of high-viscosity oil production with water and polymer solution injection. *Automation and informatization of the fuel and energy complex*, 7(612), pp. 51–60. (In Russ.)

Tadayoni M., Khalilbeyg M., Bin Junin R. (2020). A new approach to heterogeneity analysis in a highly complex carbonate reservoir by using borehole image and conventional log data. *Journal of Petroleum Exploration*

and Production Technology, 10, pp. 2613–2629. <https://doi.org/10.1007/s13202-020-00930-4>

Tudvachev A.V., Konosavsky P.K. (2013). Analysis and forecasting of phase permeability function dependencies of oil-saturated reservoirs on the example of fields of Surgut and Vartovskiy vaults of West Siberian oil and gas province. *Bulletin of St. Petersburg University. Earth Sciences*, 1, pp. 31–41. (In Russ.)

Vashakidze N.S., Filippova G.V., Raush N.L., Osipov G.S. (2024). Introduction to the assessment of the quality of cluster analysis. *International Journal of Humanities and Natural Sciences*, 10–2(97), pp. 86–89. (In Russ.) <https://doi.org/10.24412/2500-1000-2024-10-2-86-89>

Yekta A.E., Manceau J., Gabreau S., Pichavant M., Audigane P. (2018). Determination of hydrogen–water relative permeability and capillary pressure in sandstone: application to underground hydrogen injection in sedimentary formations. *Transport in Porous Media*, 122(2), pp. 333–356. <https://doi.org/10.1007/s11242-018-1004-7>

Zakirov E.S., Indrupskiy I.M., Vasiliev I.V., Anikeev D.P., Tsagan-Mandzhiev T.N. Rodionov A.E., Lachugin D.S., Afanasyev V.S., Afanasyev S.V., Antonovich A.A. (2017). Conducting comprehensive studies to assess the relative phase permeabilities for oil and water and the displacement efficiency under conditions of abnormally low reservoir injectivity (part 2). *Oil Industry*, 10, pp. 90–93. (In Russ.) <https://doi.org/10.24887/0028-2448-2017-10-90-93>

About the Authors

Sergey N. Krivoschekov – Cand. Sci. (Engineering), Associate Professor, Perm National Research Polytechnic University

29 Komsomolsky pr., Perm, 614990, Russian Federation

e-mail: krivoshchekov@gmail.com

Alexander A. Kochnev – Cand. Sci. (Engineering), Perm National Research Polytechnic University

29 Komsomolsky pr., Perm, 614990, Russian Federation

e-mail: sashakoch93@gmail.com

Evgeny S. Ozhgibesov – Assistant, Perm National Research Polytechnic University

29 Komsomolsky pr., Perm, 614990, Russian Federation

e-mail: ozhgibesov2015@yandex.ru

Dmitry O. Shirinkin – Junior Researcher, Perm National Research Polytechnic University

29 Komsomolsky pr., Perm, 614990, Russian Federation

e-mail: shirinkindo.40@mail.ru

Aleksey L. Yuzhakov – Cand. Sci. (Engineering), Associate Professor, Perm National Research Polytechnic University,

29 Komsomolsky pr., Perm, 614990, Russian Federation

e-mail: uzual94@gmail.com

*Manuscript received 1 April 2025;
Accepted 3 September 2025; Published 20 December 2025*